processes

MDPI

Article

Efficient Preparation and Bioactivity Evaluation of Aglycone Soy Isoflavones via a Multi-Enzyme Synergistic Catalysis Strategy

Yating Zhao [1], Yanhong Fu [2], Peng Du [1], Nan Li [1], Yaru Lv [1], Lizhen Hao [2], Wenlong Liu [2] and Jing Xiao [1,*]

[1] State Key Laboratory of Green Papermaking and Resource Recycling, Qilu University of Technology, Jinan 250353, China; zhaoyating0904@163.com (Y.Z.); dp0522@qlu.edu.cn (P.D.); linan1166@163.com (N.L.); lvyaru230@163.com (Y.L.)

[2] Shandong Loncote Enzymes Co., Ltd., Linyi 276000, China; fuyanhong@longda-enzyme.com (Y.F.); haolizhen@longda-enzyme.com (L.H.); ldsw66636@longda-enzyme.com (W.L.)

* Correspondence: xiaojing8168@163.com

Abstract: Aglycone-type soy isoflavones, recognized for their bioactive phytoestrogen properties, face industrial limitations due to their low natural abundance and inefficient conversion. This study optimized a multi-enzyme synergistic catalysis system using soybean sprout powder, achieving high conversion rates and purity through response surface methodology. The optimal enzyme system comprised β-glucosidase (25 U/mL), cellulase (200 U/mL), hemicellulase (400 U/mL), and β-galactosidase (900 U/mL) at pH 5.0, 50 °C, and 3.2 h. This system yielded an aglycone conversion rate of 92% and glycoside hydrolysis rate of 97%, outperforming single-enzyme approaches. Upon post-purification with AB-8 macroporous resin, the product reached a purity of 58.1 ± 0.54% and exhibited strong antioxidant activity, with DPPH and ABTS radical scavenging rates of 81.01 ± 0.78% and 71.37 ± 1.01%, respectively. In a zebrafish central nervous system injury model induced by mycophenolate mofetil, the 500 μg/mL sample group significantly reduced neural apoptosis fluorescence intensity compared to controls ($p < 0.05$), achieving a neuroprotective rate of 76.58%, which was similar to the effect of L-reducing glutathione. This study offers an efficient, cost-effective enzymatic strategy for producing aglycone soy isoflavones, highlighting their potential in functional foods and neuroprotective applications.

Keywords: aglycone-type soy isoflavones; multi-enzyme system; soybean germ powder; bioactivity

check for updates

Academic Editor: Tiago L. Albuquerque

Received: 7 May 2025
Revised: 4 June 2025
Accepted: 5 June 2025
Published: 10 June 2025

Citation: Zhao, Y.; Fu, Y.; Du, P.; Li, N.; Lv, Y.; Hao, L.; Liu, W.; Xiao, J. Efficient Preparation and Bioactivity Evaluation of Aglycone Soy Isoflavones via a Multi-Enzyme Synergistic Catalysis Strategy. *Processes* **2025**, *13*, 1831. https://doi.org/10.3390/pr13061831

Copyright: © 2025 by the authors. Licensee MDPI, Basel, Switzerland. This article is an open access article distributed under the terms and conditions of the Creative Commons Attribution (CC BY) license (https://creativecommons.org/licenses/by/4.0/).

1. Introduction

Soy isoflavones, a class of flavonoid compounds, are secondary metabolites synthesized during soybean growth that are primarily found in seed coats, hypocotyls, and cotyledons [1,2]. Structurally similar to estrogen, they act as phytoestrogens [3]. The 12 identified components of soy isoflavones are primarily categorized as bound glycoside soy isoflavones and free aglycone soy isoflavones [4]. Over 95% of soy isoflavones naturally occur as glycosides, while aglycones comprise only 2–3%. Intestinal microorganisms hydrolyze glycoside soy isoflavones into their corresponding aglycone forms before they are absorbed by the body [5–7].

Aglycone soy isoflavones demonstrate superior bioactivity compared to their glycoside counterparts [8,9]. Conversion methods include acid, alkali, and enzymatic hydrolysis. However, the acid and alkali hydrolysis processes produce many by-products and are not environmentally friendly [10,11], whereas enzymatic hydrolysis offers mild reaction conditions [12] with high efficiency and specificity [13]. Studies have primarily focused

on β-glucosidase for glycoside hydrolysis, achieving 60% conversion. Silva et al. adopted a hemicellulase-assisted β-glucosidase conversion method, increasing the aglycone soy isoflavone concentration by 40% in soy milk [14]. Due to the high cost of β-glucosidase [15] and the limited research on other hydrolases, new, cost-effective, and efficient compound enzyme formulas are needed.

Soy isoflavone hydrolysis generates various by-products, necessitating further separation and purification for high-purity aglycone-type soy isoflavones [16]. Purification methods include solid-phase extraction, column chromatography, resin adsorption, and membrane separation [17–20]. In particular, renewable macroporous resin adsorption is effective, simple, and cost-efficient for industrial production [21–24].

Aglycone-type soy isoflavones exhibit antioxidant, anticancer, osteoprotective, and neuroprotective properties [20–28]. Central nervous system (CNS) injuries, including stroke and neurodegeneration, are major global health concerns [24]. CNS injury is frequently associated with conditions such as hemiplegia, aphasia, intellectual disability, or even more severe outcomes like coma and death [29]. The nervous system of zebrafish closely resembles that of humans, with a similar brain morphology, myelin sheath architecture, and oligodendrocyte differentiation [30]. Accordingly, zebrafish are an ideal model for evaluating neuroprotective effects [25].

Mycophenolate mofetil (MMF), a potent, selective, noncompetitive, and reversible inhibitor of inosine monophosphate dehydrogenase (IMPDH), is extensively employed to create CNS injury models by obstructing the de novo synthesis of guanosine nucleotides, depleting guanosine nucleotides, and inhibiting DNA synthesis [26]. In zebrafish, MMF impairs neural development and causes the apoptosis of neural cells [31]. Their transparent bodies enable the rapid detection of compound-induced nervous system damage through special staining in live or intact fixed specimens.

The industrial production of aglycone soy isoflavones encounters several obstacles, such as high enzymatic costs, the limited efficiency of single enzymes, and complex purification processes. Although existing studies have attempted to improve conversion rates through microbial metabolism and chemical modification, the synergistic effects of multi-enzyme systems remain unclear. Functional evaluations targeting CNS protection predominantly rely on in vitro models, lacking in vivo validation in animal models.

This study aims to analyze the synergistic effects of β-glucosidase, cellulase, hemicellulase, and β-galactosidase using orthogonal experiments and response surface methodology, and to develop an efficient, low-consumption aglycone conversion process. Leveraging the adsorption characteristics of AB-8 macroporous resin, a highly selective purification process was established. Additionally, the neuroprotective effect and dose–response relationship of aglycone soy isoflavones were evaluated through an MMF ethyl ester-induced zebrafish CNS injury model. By overcoming the efficiency limitations of traditional single-enzyme methods, this study provides theoretical and technical support for the high-value utilization of soy by-products, offering a system for developing natural neuroprotective agents.

2. Materials and Methods

2.1. Materials and Reagents

Daidzin (D), genistin (GL), glycitin (G), daidzein (DE), genistein (GLE), and glycitein (GE) standards, as well as hemicellulase (20,000 U/g), were obtained from Shanghai Yuanye Biotechnology Co., Ltd. (Shanghai, China). β-Glucosidase (3000 U/g), cellulase (3000 U/g), and β-galactosidase (15,000 U/g) were provided by Shandong Longkote Enzyme Co., Ltd. (Linyi, China). Soybean sprout residue powder was procured from the local market. Anhydrous ethanol (high-performance liquid chromatography [HPLC] grade), methanol (HPLC grade), acetonitrile (HPLC grade), disodium hydrogen phosphate

(AR grade), citric acid (AR grade), vitamin C (V_C; AR grade), potassium persulfate (AR grade), sodium hydroxide (AR grade), hydrochloric acid (AR grade), and acetic acid (HPLC grade) were purchased from Sinopharm Chemical Reagent Co., Ltd. (Shanghai, China). Macroporous resin (AB-8 type) was obtained from Beijing Solarbio Science & Technology Co., Ltd. (Beijing, China), while DPPH and ABTS assay kits were sourced from Beijing Coolab Technology Co., Ltd. (Beijing, China). Dimethyl sulfoxide and acridine orange were acquired from Shanghai Macklin Biochemical Co., Ltd. (Shanghai, China) Mycophenolic acid morpholino ethyl ester was provided by Shanghai Aladdin Biochemical Technology Co., Ltd. (Shanghai, China). L-Reduced glutathione (hereafter referred to as glutathione) was purchased from Sigma-Aldrich (Shanghai) Trading Co., Ltd. (Shanghai, China).

Instruments used in this study included two analytical balances (TLE204E, Shanghai Yuanxi Instruments Co., Ltd. (Shanghai, China); CP214, OHAUS Corporation, Parsippany, NJ, USA) and an electric thermostatic water bath (DK-S26, Shanghai Changken Laboratory Equipment Co., Ltd., Shanghai, China), desktop water bath shaker (DSHZ-300, Taicang Qiangle Laboratory Equipment Co., Ltd., Taicang, China), UV-Vis spectrophotometer (NanoPhotometer NP80, Implen GmbH, Munich, Germany), high-performance liquid chromatograph (LC-20AD, Shimadzu Corporation, Kyoto, Japan), dissecting microscope (SZX7, Olympus Corporation, Tokyo, Japan), CCD camera (VertA1, Shanghai Tusu Vision Technology Co., Ltd., Shanghai, China), and motorized-focus continuous zoom fluorescence microscope (AZ100, Nikon Corporation, Tokyo, Japan).

2.2. Enzymatic Hydrolysis Process of Soy Isoflavones

The soybean germ residue was ground using a grinder and passed through a sample sieve (60 mesh). The powder was homogenized, transferred to a clean container, and sealed for storage. The soybean germ powder was aliquoted into separate conical flasks, and a citric acid–sodium phosphate buffer solution with a specific pH value was added to each flask at a solid-to-liquid ratio of 1 g:10 mL.

Given that ultrasound-assisted hydrolysis significantly enhances the aglycone content post-hydrolysis due to its role in cleaving the glycosidic bonds [32], the mixtures were ultrasonicated at 70 °C for 30 min before adding the following enzymes to the flasks: β-glucosidase (30 U/mL), cellulase (200 U/mL), hemicellulase (200 U/mL), and β-galactosidase (500 U/mL). Cellulase and hemicellulase disrupt the cell walls to release soy isoflavones; β-glucosidase hydrolyzes the glycoside soy isoflavone into bioactive aglycones; β-galactosidase, cellulase, and hemicellulase enhance the process's efficiency by removing interfering oligosaccharides.

The solutions were thoroughly mixed to ensure complete enzyme–substrate interaction. The reaction systems were incubated in a water bath shaker at 50 °C for 5 h to facilitate enzymatic hydrolysis. After the reaction, the mixtures were heated in a boiling water bath for 10 min to deactivate the enzymes and then cooled to room temperature (25 °C). The solutions were transferred to centrifuge tubes and centrifuged at 8000 rpm for 10 min. The supernatants were collected, while the residues underwent secondary ultrasonication with 70% ethanol. Finally, the aglycone-type soy isoflavones were extracted by mixing the enzymatic hydrolysate with 80% ethanol at a volumetric ratio of 1:9 (v/v).

2.3. Condition Optimization for Preparing Aglycone Soy Isoflavones Using Composite Enzymes

To optimize the composite enzyme ratios, the yield of aglycone soy isoflavones served as the evaluation index. The experiments were conducted under the following specific conditions: pH 5.0, 50 °C, solid-to-liquid ratio of 1 g/10 mL, and reaction time of 5 h. The enzymatic formulation was optimized by varying the concentrations of the hydrolytic enzymes as follows: β-glucosidase (10, 15, 20, 25, and 30 U/mL), cellulase (100, 150, 200,

250, and 300 U/mL), hemicellulase (100, 200, 400, 600, and 800 U/mL), and β-galactosidase (100, 300, 500, 700, and 900 U/mL).

Once the enzyme formulation was finalized, a further optimization of the following reaction conditions was performed: pH (4.4, 4.6, 4.8, 5.0, 5.2, and 5.4), temperature (35, 40, 45, 50, 55, and 60 °C), and reaction time (0.5, 1, 3, 5, 7, and 9 h). Significant factors identified through single-factor experiments led to the selection of pH (A), reaction time (B), and reaction temperature (C) as the key independent variables. The aglycone conversion rate (Y) was used as the response value. A Box–Behnken design (BBD) with three factors and three levels was applied to develop a response surface model.

2.4. Aglycone Soy Isoflavone Purification Process

Under ambient temperature conditions, 20 mL of crude aglycone soy isoflavone extract was adjusted to different pH values (5.0, 5.5, 6.0, 6.5, and 7.0) and loaded onto a chromatography column packed with pre-conditioned AB-8 macroporous resin. The adsorption process was conducted for varying durations (2, 4, 6, 8, and 10 h), followed by washing with deionized water. Elution was performed using ethanol solutions of varying concentrations (40%, 50%, 60%, 70%, and 80%) and pH values (4.5, 5.0, 5.5, 6.0, and 6.5). After a set period of static desorption (1, 3, 5, 7, and 9 h), the eluate was collected and diluted to 100 mL. The eluate was analyzed using HPLC. Each experimental group was repeated thrice. The adsorption rate was used as the evaluation index to optimize the pH and adsorption time, while the desorption rate was used to optimize the ethanol concentration, pH, and adsorption time. The formulas for calculating the adsorption and desorption rates are provided in Equations (1) and (2), respectively:

$$A = \frac{(C_0 - C_1)}{C_1} \times 100 \quad (1)$$

$$D = \frac{C_2}{(C_0 - C_1)} \times 100 \quad (2)$$

where A represents the adsorption rate (%); D is the desorption rate; C_0 represents the concentration of aglycone soy isoflavones in the adsorbed pre-sample (μg/mL); C_1 is the concentration of aglycone soy isoflavones in the sample solution after adsorption (μg/mL); and C_2 represents the concentration of aglycone-type soy isoflavones in the desorption solution (μg/mL).

Based on single-factor experiments, orthogonal experiments were performed to determine the optimal purification conditions. The aglycone soy isoflavone samples were concentrated and dried under these optimal conditions; purity was calculated using Equation (3):

$$P = \frac{C_3 \times V \times 10^{-3}}{m} \times 100 \quad (3)$$

where P is the purity (%); C_3 represents the mass concentration of the aglycone-type soybean isoflavone sample (μg/mL); V is the constant volume (mL); and m represents the quality of the aglycone-type soybean isoflavone sample (mg).

2.5. Detection Method for Soy Isoflavones

HPLC qualitatively and quantitatively detected soy isoflavones through a comparison with standards.

Sample Preparation: Precisely 10.0 mg of each soy isoflavone standard was weighed and dissolved in 60% methanol to prepare individual standard stock solutions, each adjusted to a final 10 mL volume. These stocks were diluted with a 10% methanol solution

to generate a series of mixed standard solutions at varying concentrations. All standard solutions were filtered through a 0.45 μm membrane filter.

Detection: The analytical protocol was adapted from a previously reported protocol [33] with modifications to optimize detection specificity. A Shimadzu 227-30017-08 Shimpack GIST C18 chromatographic column (5 μm, 4.6 × 250 mm, Shimadzu Corporation, Kyoto, Japan) was used. The mobile phase comprised solution A (0.1% acetic acid–water solution) and solution B (0.1% acetic acid–methanol solution), with a flow rate of 1 mL/min. The injection volume was 10 μL, and the detection wavelength was 260 nm. The column temperature was maintained at 35 °C. The gradient elution program for the mobile phase is detailed in Table S1.

Quantification: Calibration curves were created by plotting the mass concentration of each soy isoflavone component on the *x*-axis and the peak area on the *y*-axis. The regression equations and correlation coefficients (R^2) are presented in Table S2. A specific amount of the aglycone soy isoflavone extract was filtered through a 0.45 μm membrane and analyzed by HPLC. Qualitative analysis was based on retention time, and the content of each component was determined by substituting the peak area into the regression equation. The hydrolysis rate of glycoside soy isoflavones and the yield of aglycone soy isoflavones were calculated using Equations (4) and (5), respectively:

$$H = \frac{M_1 - M_2}{M_1} \times 100 \quad (4)$$

$$Y = \frac{M_3 - M_4}{M_1} \times 100 \quad (5)$$

where H represents the hydrolysis rate of glycosidic soybean isoflavones (%); Y is the yield of aglycone soy isoflavones (%); M_1 is the total amount of glycoside soybean isoflavones before enzymatic hydrolysis (μg); M_2 represents the total amount of glycoside soybean isoflavones after enzymatic hydrolysis (μg); M_3 is the total amount of aglycone soy isoflavones after enzymatic hydrolysis (μg); and M_4 represents enzymatic hydrolysis of the total amount of pre-aglycone soy isoflavones (μg).

2.6. In Vitro Antioxidant Activity Determination

2.6.1. DPPH Free Radical Scavenging Rate

The radical scavenging activity of DPPH was determined using the protocol described by Kim et al. [34] with a slight modification. Briefly, dried powder aglycone soy isoflavone samples and V_C at a certain concentration were prepared. The sample solution was mixed with a 0.1 mmol/L DPPH solution in equal proportions and was allowed to stand at room temperature (25 °C) in the dark for 30 min; absorbance (A_1) was measured at 517 nm. Similarly, the sample solution was mixed with anhydrous ethanol in equal proportions, and was allowed to stand at room temperature in the dark for 30 min; absorbance (A_2) was measured at 517 nm. Additionally, anhydrous ethanol was mixed with a 0.1-mmol/L DPPH solution in equal proportions, and was left to stand at room temperature in the dark for 30 min; absorbance (A_3) was measured at 517 nm. The DPPH free radical scavenging rate of the sample was calculated using Equation (6):

$$DPPH\ radical\ scavenging\ rate = \frac{A_3 - (A_1 - A_2)}{A_3} \times 100\% \quad (6)$$

where A_1 represents the sample solution + absorbance of the DPPH solution; and A_2 is the sample solution + absorbance of water; A_3 is the water (ethanol) + absorbance of the DPPH solution.

2.6.2. ABTS Radical Scavenging Rate

The ABTS radical scavenging assay was performed as per the protocols described by Lee et al. [35] with slight modifications. An aqueous solution of 7 mmol/L ABTS was combined in equal parts with a 2.45 mmol/L $K_2S_2O_8$ aqueous solution and kept in the dark to react for 12–16 h. The reaction mixture was diluted 40-fold with anhydrous ethanol to produce ABTS radicals. A 200 µL sample solution was mixed with 4 mL of the ABTS working solution and incubated in the dark at room temperature (25 °C) for 10 min; absorbance (A_1) was measured at 734 nm. For the blank, distilled water replaced the sample solution; absorbance (A_2) was measured at 734 nm. The ABTS radical scavenging activity was calculated using Equation (7):

$$ABTS\ radical\ scavenging\ rate = \frac{A_2 - A_1}{A_2} \times 100\% \quad (7)$$

where A_1 represents the sample solution + absorbance of the ABTS working solution; A_2 is the water (ethanol) + absorbance of the ABTS working solution.

2.7. Evaluating Central Nervous System-Protective Effects in Zebrafish

2.7.1. Sample Solution Preparation

Aglycone soy isoflavone sample solution: A 0.20 g aglycone soy isoflavone sample was weighed and dissolved in deionized water and diluted to a total volume of 100 mL. Subsequently, a series of mixed standard solutions with varying mass concentrations was prepared through stepwise dilution to final concentrations of 125, 250, 500, 1000, and 2000 µg/mL.

Aglycone soy isoflavone standard solution: The aglycone soy isoflavone standard was dissolved in deionized water and diluted to a total volume of 100 mL to obtain a 500 µg/mL solution.

Positive control (L-reduced glutathione): A 0.0615 g sample of L-reduced glutathione (GSH) was weighed and dissolved in deionized water, and then diluted to a total volume of 100 mL to prepare a 615 µg/mL solution.

2.7.2. Animals and Treatments

All zebrafish experiments were conducted as per protocols approved by the Animal Protection and Use Committee of the Qilu University of Technology (Approval No. 2024-003) and were approved by the Animal Ethics Committee of the Qilu University of Technology. The experimental animal use license number was SYXK (Zhejiang) 2022-0004, and husbandry management complied with the requirements of international AAALAC accreditation (Accreditation No. 001458).

The zebrafish were maintained in fish water at 28 °C, with a water quality of 200 mg of instant sea salt added per 1 L of reverse osmosis water, with a conductivity of 450–550 µS/cm, a pH of 6.5–8.5, and a hardness of 50–100 mg/L $CaCO_3$. The breeding system was set up as a 14 h/10 h light/dark cycle.

2.7.3. Maximum Test Concentration (MTC) Determination

Wild-type AB zebrafish were randomly selected 1 day post-fertilization (1 dpf) and placed in 6-well plates, with 30 zebrafish per well for the experimental group. Samples were administered in 125, 250, 500, 1000, and 2000 µg/mL water solutions. Concurrently, a normal control group and a model control group were established, with 3 mL per well. All experimental groups, excluding the control group, were administered 0.25 µmol/L MMF in a water solution to induce CNS injury. Following 1 day of treatment at 28 °C, the MTCs of the samples were determined.

2.7.4. Protective Effect on CNS Injury

Thirty wild-type AB zebrafish (1 dpf) were placed in 6-well plates with 3 mL per well. Excluding the normal control group, all groups received MMF in a water solution to establish the zebrafish CNS injury model. The positive control group was administered 615 μg/mL glutathione. The model control group did not receive any drug treatment. The experimental groups were administered 125, 250, and 500 μg/mL samples. After treatment at 28 °C for 1 day, acridine orange (AO) staining was conducted. Following staining, ten zebrafish were randomly selected from each experimental group. The samples were imaged and photographed using a fluorescence microscope. The data collection and analysis were carried out using the NS-Elements SD3.20 advanced image processing software to assess the fluorescence intensity of apoptosis in the zebrafish nerve axis cells. The protective efficacy of the samples on the CNS was evaluated based on a statistical analysis of this index. The protection rate of the CNS was calculated according to Equation (8):

$$P = \frac{S_1 - S_3}{S_1 - S_2} \times 100 \quad (8)$$

where P is the CNS protection rate (%); S_1 represents the fluorescence intensity of neural axonal cell apoptosis in the model control group; S_2 is the fluorescence intensity of neural axonal cell apoptosis in the normal control group; and S_3 represents the fluorescence intensity of neural axonal cell apoptosis in the sample group.

2.8. Statistical Analysis

Each sampling dataset was replicated at least thrice. Statistical analysis was conducted using one-way analysis of variance (ANOVA), followed by a Tukey post hoc test. Graphs were created using Origin 8.5 software. Experimental data are reported as mean ± standard deviation (SD), with $p < 0.05$ set as the criterion for statistical significance.

3. Results and Discussion

3.1. Composite Enzyme Ratio Optimization

Based on previous studies on soy isoflavone hydrolysis by various enzymes, β-glucosidase (100 U/g, 3000 U/g), cellulase (3000 U/g, 50,000 U/g), hemicellulase (20,000 U/g), β-galactosidase (10,000 U/g, 150,000 U/g), and snailase (921 U/g) were evaluated. The aglycone soy isoflavone yield served as the evaluation criterion. The optimal enzyme combination was β-glucosidase (3000 U/g), cellulase (3000 U/g), hemicellulase (20,000 U/g), and β-galactosidase (10,000 U/g).

Soybean germ powder was hydrolyzed using composite enzymes. The optimal enzyme combination was identified as $A_2B_2C_2D_3$, corresponding to the following enzyme concentrations: β-glucosidase (25 U/mL), cellulase (200 U/mL), hemicellulase (400 U/mL), and β-galactosidase (900 U/mL) (Table 1). The multifactorial ANOVA results revealed that β-glucosidase exhibited the highest F-value, indicating its predominant influence on the aglycone soy isoflavone yields compared to cellulase, hemicellulase, and β-galactosidase (Table 2). This predominance is attributed to the high substrate specificity of β-glucosidase in hydrolyzing 1,4-glycosidic bonds, a reaction that directly catalyzes the conversion of glycosylated soy isoflavones into their aglycone forms [35].

Table 1. Compound enzyme formulation outcomes.

No.	A: β-Glucosidase (U/mL)	B: Cellulase (U/mL)	C: Hemicellulase (U/mL)	D: β-Galactosidase (U/mL)	Aglycone Soy Isoflavone Yield (%)
1	1 (20)	1 (150)	1 (200)	1 (500)	82.57
2	1	2 (200)	2 (400)	2 (700)	85.29
3	1	3 (250)	3 (600)	3 (900)	83.57
4	2 (25)	1	2	3	88.62
5	2	2	3	1	89.68
6	2	3	1	2	87.42
7	3 (30)	1	3	2	85.85
8	3	2	1	3	87.09
9	3	3	2	1	86.63
K1	251.43	257.04	257.08	258.88	
K2	265.72	262.06	260.54	258.56	
K3	259.57	257.62	259.1	259.28	
k_1	83.81	85.68	85.693	86.293	
k_2	88.573	87.353	86.847	86.187	
k_3	86.523	85.873	86.367	86.427	

Table 2. Analysis of variance (ANOVA) results.

Source	Sum of Squares	df	Mean Squares	F-Value	*p*-Value
Intercept	197,939.741	1	197,939.741	506,148.652	<0.01 **
β-glucosidase	99.411	2	49.706	127.102	<0.01 **
Cellulase	15.544	2	7.772	19.873	<0.01 **
Hemicellulase	5.974	2	2.987	7.638	<0.01 **
β-galactosidase	0.367	2	0.184	0.470	0.633
Residual	7.039	18	0.391		

Note: ** $p < 0.01$.

Based on the optimal conditions derived from the orthogonal experiments, three parallel verification experiments were conducted. The average conversion rate of the aglycone soy isoflavones was 90.79 ± 0.38%, and the hydrolysis rate of glycosylated soy isoflavones reached 93.56% ± 0.82%.

3.2. Composite Enzyme Reaction Condition Optimization

3.2.1. Analysis of Single-Factor Experiment Results

pH is a critical factor affecting enzymatic hydrolysis. The aglycone soy isoflavone yield increased from 64.11 ± 0.80% to 85.13 ± 1.59% when the pH was raised from 4.4 to 5.0 (Figure 1A). Further increases in pH deviated from the optimal range for enzyme activity. Such deviations disrupted the optimal microenvironment for enzyme–substrate interactions, reducing enzyme activity and decreasing the aglycone soy isoflavone yield. A pH of 5.0 represented an optimal condition for enzymatic soybean germ powder hydrolysis, achieving a high aglycone isoflavone yield of 85.13 ± 1.59%.

Over a 1–9 h reaction period, the aglycone soy isoflavone yield increased rapidly during the initial phase due to high substrate availability and low product concentration, driving the reaction forward (Figure 1B). After 3 h, substrate depletion and product inhibition caused the reaction to plateau, stabilizing the yield at 66.79 ± 0.26%. Therefore, 3 h was selected as the optimal reaction time.

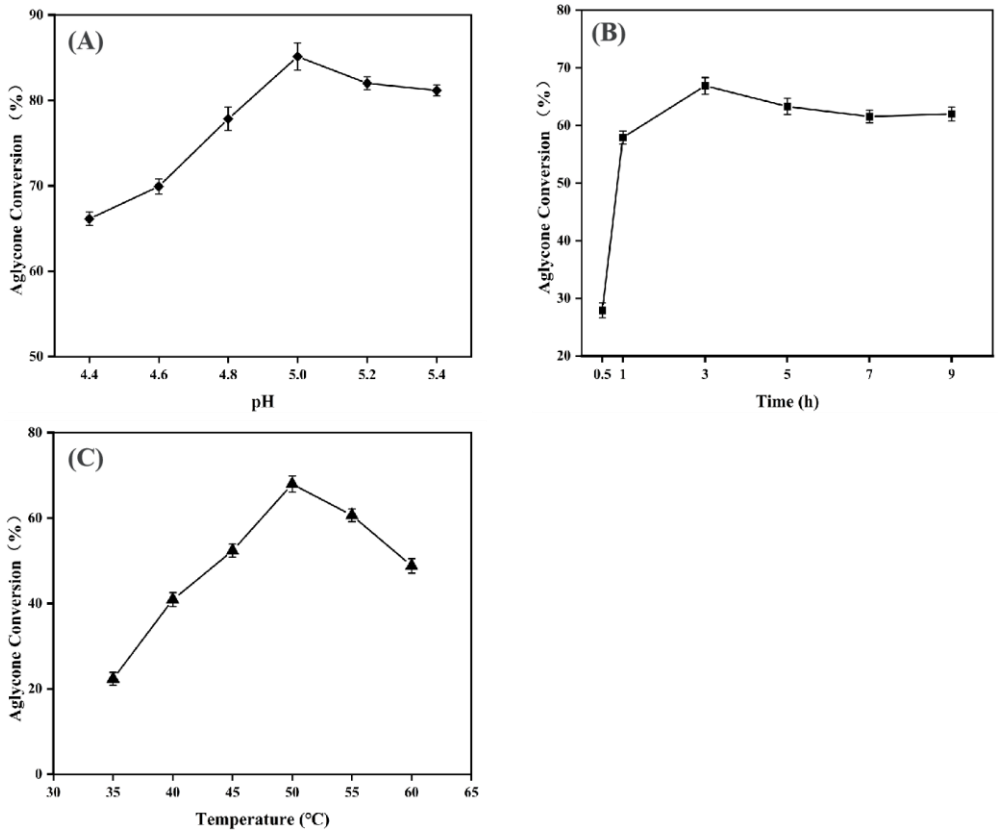

Figure 1. Effect of different enzyme hydrolysis conditions on aglycone conversion: (**A**) pH, (**B**) hydrolysis time, and (**C**) temperature.

Additionally, as the reaction temperature increased from 35 °C to 50 °C, the yield progressively rose (Figure 1C). Elevated temperatures enhanced enzymatic activity and molecular collision frequency, improving enzyme–substrate interactions. The maximum yield of 68.83 ± 2.44% was achieved at 50 °C. Beyond this temperature, enzyme denaturation, due to protein thermal instability, sharply reduced their activity. Hence, 50 °C was determined as the optimal reaction temperature. Based on the results of the single-factor analysis, the optimal reaction conditions were as follows: pH 4.8–5.2, reaction time 1–5 h, and reaction temperature 45–55 °C.

3.2.2. Response Surface Model Validation and Optimal Parameters

The response surface experimental design was implemented using Design-Expert 13.0 software (Table 3). A multiple regression analysis of the experimental data yielded a predictive second-order polynomial equation describing the relationship between the response variable and independent variables:

$$Y = 91.62 + 1.79A + 0.6962B + 0.985C - 0.6625AB - 1.29AC - 0.71BC - 4.30A^2 - 2.15B^2 - 4.02C^2$$

where Y represents the yield of aglycone soy isoflavones (%); A, B, and C represent pH, reaction time, and reaction temperature, respectively. The terms AB, AC, and BC represent the interaction effects between pH and reaction time, pH and reaction temperature, and reaction time and reaction temperature, respectively.

Table 3. Experimental design and results.

Sequence	Three Factors with Three Levels			Response Values
	A: pH	B: Time (h)	C: Temperature (°C)	Aglycone Conversion (%)
1	5.2	5	50	86.77
2	5	5	45	86.12
3	4.8	3	45	78.85
4	4.8	1	50	82.23
5	5.2	1	50	86.78
6	5	5	55	86.24
7	5	3	50	92.05
8	5	1	55	86.19
9	5.2	3	45	85.34
10	4.8	3	55	83.82
11	5	3	50	91.58
12	5	3	50	91.47
13	5	3	50	91.19
14	5	3	50	91.82
15	5.2	3	55	85.17
16	4.8	5	50	84.87
17	5	1	45	83.23

ANOVA was performed to evaluate model significance (Table S3). The model exhibited an F-value of 169.80 ($p < 0.0001$), confirming its statistical significance. A non-significant lack-of-fit term validated the model's reliability. Based on F-values, the factors influencing aglycone conversion efficiency were ranked as follows: pH > reaction temperature > reaction time (FA > FC > FB). The adjusted coefficient of determination ($RAdj^2$ = 0.9896) further demonstrated excellent agreement between the experimental data and the polynomial model.

The interactions between experimental factors on the aglycone soy isoflavone yield were evaluated using response surface plots and contour plots (Figure 2). The steepness of the response surface plots indicates the degree of influence on the aglycone soy isoflavone yield: the steeper the slope, the greater the impact, while a gentler slope indicates a smaller effect. In the contour plots, an elliptical shape suggests a greater influence on the yield, whereas a circular shape indicates a smaller influence. The interactions between pH and reaction temperature, as well as between reaction time and reaction temperature, were significant. Additionally, the combination of pH and reaction temperature impacted the yield.

The Design-Expert 13.0 software predicted the following optimal hydrolysis conditions: pH 5.037, a reaction time of 3.239 h, and a temperature of 50.410 °C, as well as an estimated aglycone soy isoflavone yield of 91.87%. To validate this prediction, triplicate experiments were conducted under slightly adjusted conditions (pH 5.0, 3.2 h, 50.0 °C). The actual average aglycone soy isoflavone yield was 92.02 ± 0.76%, exceeding the theoretical prediction.

Traditional studies primarily rely on a single β-glucosidase to catalyze the hydrolysis of glycoside soy isoflavones into aglycone soy isoflavones. For example, Macedo et al. [33] reported a twofold increase in the aglycone concentration in soymilk using β-glucosidase, although the conversion remained limited due to single-enzyme catalysis. In this study, a combination of β-glucosidase (25 U/mL), cellulase (200 U/mL), hemicellulase (400 U/mL), and β-galactosidase (900 U/mL) was employed. Through orthogonal experiments and response surface optimization, the aglycone soy isoflavone yield increased to 92.02 ± 0.76%, with a glycoside hydrolysis rate of 97.07 ± 0.95%, representing an improvement of over 30% compared to that of single-enzyme methods. This result significantly outperformed

the acid hydrolysis method reported by Lee et al. [11] (hydrolysis rate: ~75%) and the single β-glucosidase method reported by Otieno et al. [15] (hydrolysis rate: 82%).

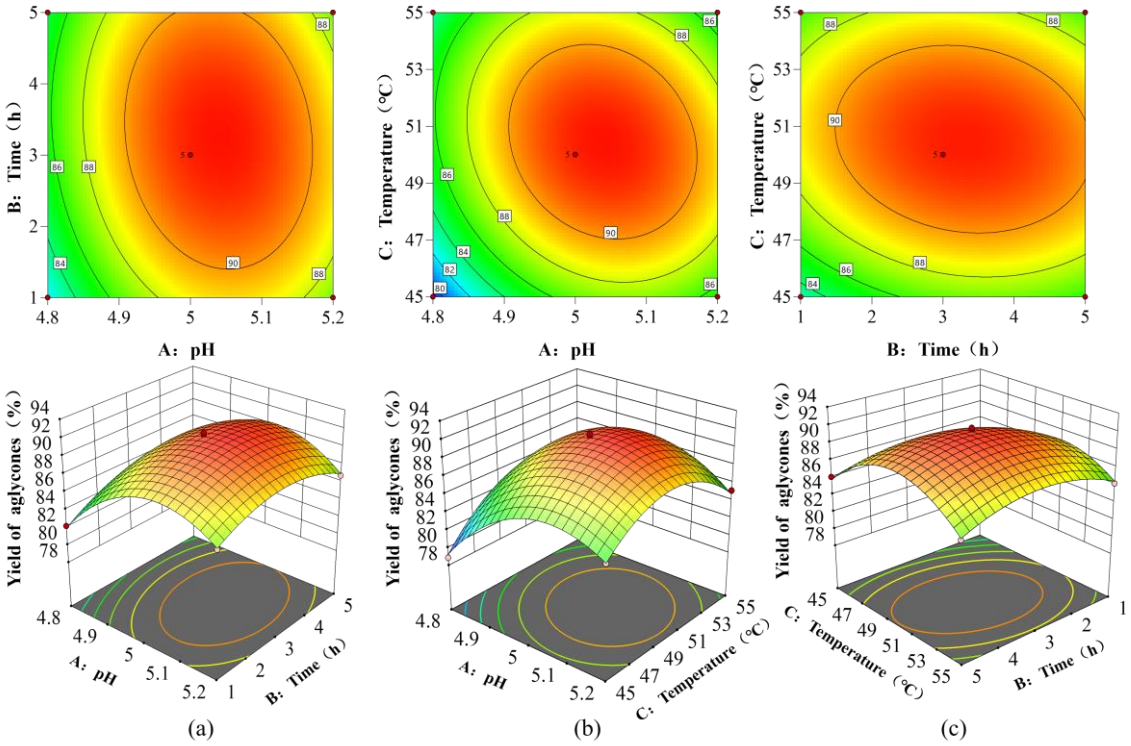

Figure 2. Response surface and contour map of interactive effects between different factors. (**a**) Interaction between pH and hydrolysis time; (**b**) interaction between pH and temperature; and (**c**) interaction between hydrolysis time and temperature.

3.3. Purification Results of Aglycone Soy Isoflavones

3.3.1. Effects of Different Adsorption Conditions on Adsorption Rate

For the crude extract following hydrolysis, the adsorption rate initially increased and then decreased as the pH level rose from 5.0 to 7.0 (Figure 3A). This is attributed to the hydrogen bonding mechanism between the phenolic hydroxyl groups of aglycone soy isoflavones (weakly acidic due to their molecular structure) and the adsorption sites on the AB-8 macroporous resin. Weakly acidic conditions (pH 6.0) maximized this interaction, achieving a peak adsorption efficiency of 80.83 ± 0.55%. Beyond pH 6.0, the reduced acidity weakened resin–substrate binding, leading to a sharp decline in adsorption efficiency.

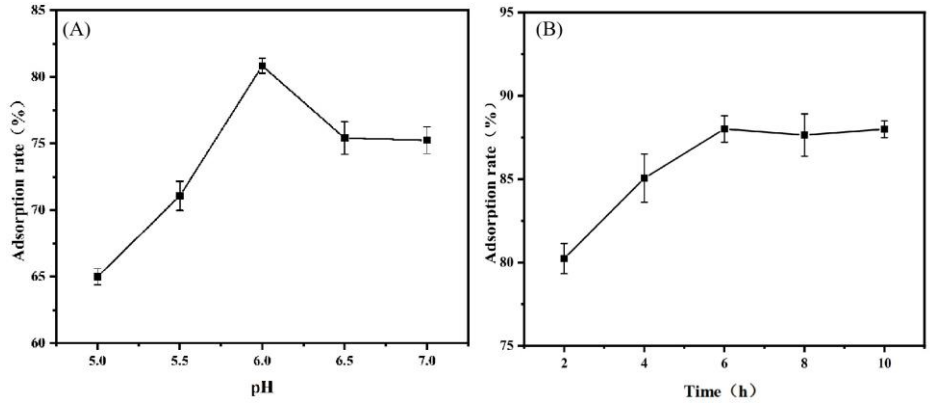

Figure 3. Effect of different adsorption conditions on adsorption rate: (**A**) pH and (**B**) time.

Under a pH of 6.0, the adsorption rate rapidly increased with an extended adsorption time from 2 to 10 h (Figure 3B). At an adsorption time of 2 h, the brief contact period between the crude extract and macroporous resin resulted in the elution of aglycone soy isoflavones in the sample solution before being fully absorbed. This led to the lowest adsorption rate (80.03 ± 1.29%). When the adsorption time reached 6 h, the adsorption rate increased to 88.11 ± 0.97%. Hence, sufficient adsorption time allows more aglycone soy isoflavones to be adsorbed by the macroporous resin. Beyond 6 h, adsorption plateaued, indicating that an equilibrium was reached. Thus, 6 h was identified as the optimal adsorption duration.

3.3.2. Influence of Different Desorption Conditions on Desorption Rate

Single-factor experiments revealed that ethanol concentration, pH, and desorption time significantly influenced the desorption efficiency of aglycone soy isoflavones. Desorption efficiency significantly increased as ethanol concentration rose from 40% to 70%, reaching 83.08 ± 0.89% (Figure 4A). This can be attributed to the reduced solvent polarity enhancing the release of aglycone soy isoflavones. However, further increases in ethanol concentration led to a plateau in the desorption rate due to increased volatility. The desorption rate rose with increasing pH levels, from 4.5 to 6.0, reaching a maximum of 78.33 ± 0.31% at pH 6.0 (Figure 4B). Beyond this pH, the desorption rate declined. Additionally, extending the desorption time from 1 to 5 h increased the desorption rate from 48.86 ± 0.24% to 66.36 ± 0.47% (Figure 4C). Minimal changes were observed when the desorption time exceeded 5 h.

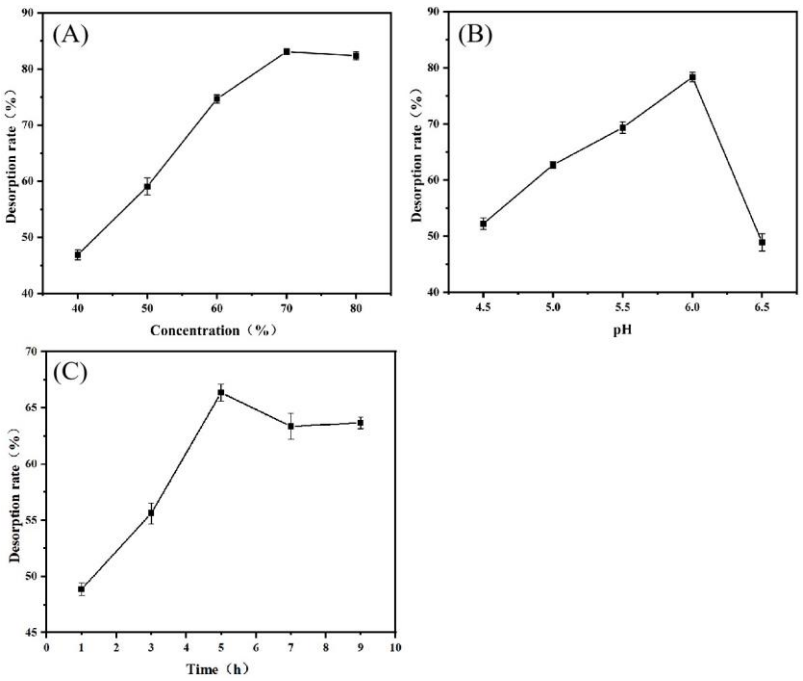

Figure 4. Effect of different desorption conditions on desorption rate: (**A**) ethanol concentration, (**B**) pH, and (**C**) time.

Based on these results, desorption was performed under the following optimized conditions: 70% ethanol concentration as the desorption solution, pH 6.0, and a desorption time of 5 h. Three parallel experiments conducted under these conditions yielded an average desorption rate of 79.13 ± 0.53%.

3.3.3. Effects of Multi-Enzyme Synergistic Catalysis and Purification on Aglycone Soy Isoflavones

The glycoside and aglycone soy isoflavone contents changed significantly after undergoing multi-enzyme synergistic catalysis and purification. The glycoside soy isoflavone content in the soybean sprout powder was markedly higher than that of aglycone soy isoflavones (Figure 5A). Following enzymatic hydrolysis, the absorption peak intensities for daidzin, genistin, and glycitein decreased significantly or disappeared, while the absorption peak intensities of daidzein, genistein, and glycitein aglycones increased sharply. Hence, the enzyme complex elicited a remarkable hydrolysis effect. After purification, the aglycone soy isoflavone purity increased to 58.1 ± 0.35%. The remaining ~41.9% of the non-aglycone fraction contained primarily glycoside isoflavones and hydrolysis by-products (e.g., polysaccharides), with trace amounts of incompletely adsorbed aglycone soybean isoflavones. Future purification studies should focus on integrating multiple purification techniques (e.g., crystallization and membrane filtration) to enhance the purity of the aglycone products and isolate distinct soy isoflavone fractions. This multidimensional approach will maximize bioefficacy by eliminating interfering glycosylated isoforms and impurities.

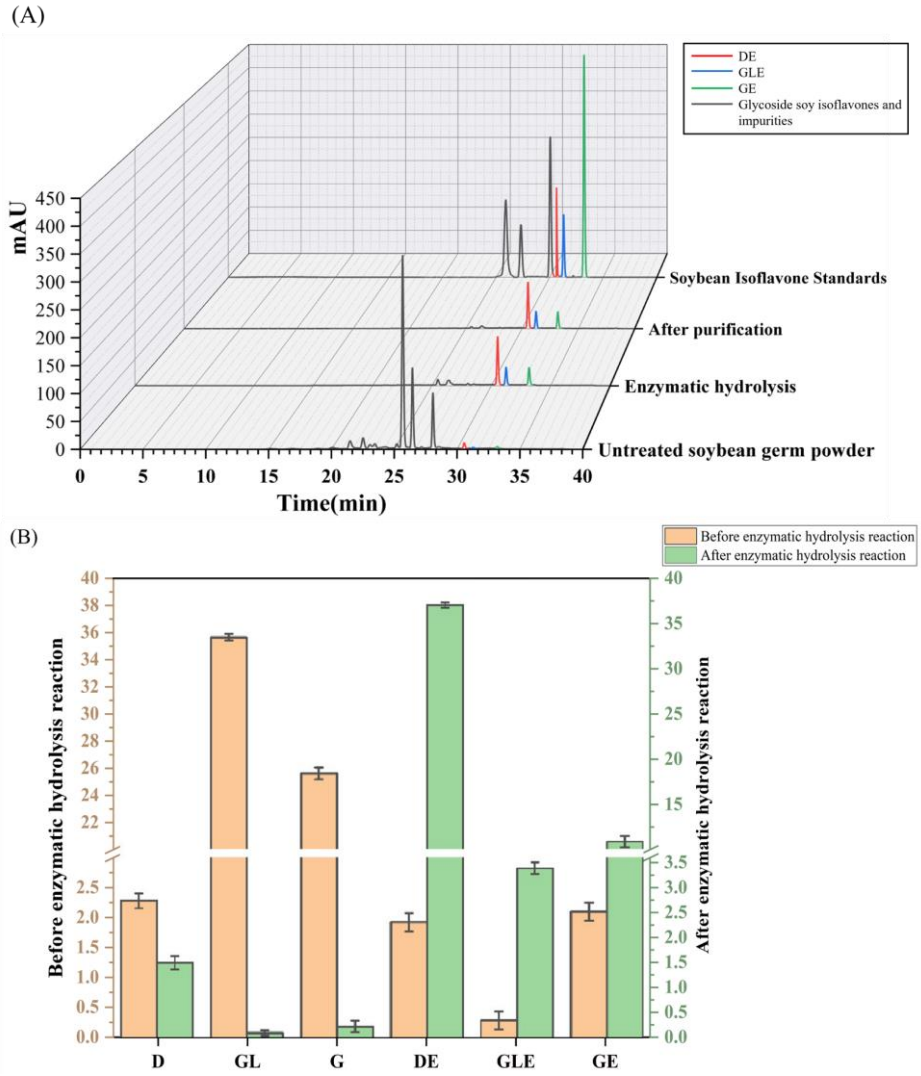

Figure 5. Changes in soy isoflavone components before and after processing. (**A**) High-performance liquid chromatography profiles; (**B**) changes in the content of six soy isoflavones.

The changes in soy isoflavone components before and after enzymatic hydrolysis were calculated using the calibration equations of the standard curves for soy isoflavone components alongside the peak areas of each component (Figure 5B). Before enzymatic hydrolysis, the glycoside soy isoflavone content was 93.77 ± 0.11%, while the aglycone soy isoflavone content was 6.23 ± 0.27%. After enzymatic hydrolysis and purification, the aglycone soy isoflavone content increased to 96.49 ± 0.05%.

3.4. Evaluation of Aglycone Soy Isoflavone Bioactivity

3.4.1. In Vitro Antioxidant Activity

Free radicals can extract electrons from biomolecules, leading to alterations that contribute to various diseases, including inflammation, aging, and cardiovascular diseases. These free radicals can react with hydrogen donors (e.g., phenolic compounds), and antioxidant capacity can be indicated by color changes, with V_C as a positive control.

As the concentration increased, the aglycone soy isoflavone ethanol solutions exhibited increasing trends in both antioxidant assays, reaching a plateau (Figure 6). At 80 μg/mL, the scavenging rate of DPPH radicals reached 81.01 ± 0.14%. Similarly, at 70 μg/mL, the scavenging rate of ABTS radicals was 71.37 ± 0.41%, significantly higher than that reported for individual aglycone soy isoflavones (e.g., scavenging rate of daidzein: ~65%) [29,30]. Compared to that of synthetic antioxidants, such as V_C, the scavenging rate of aglycone products was slightly lower. However, their natural origin makes them more suitable for the food and health product sectors.

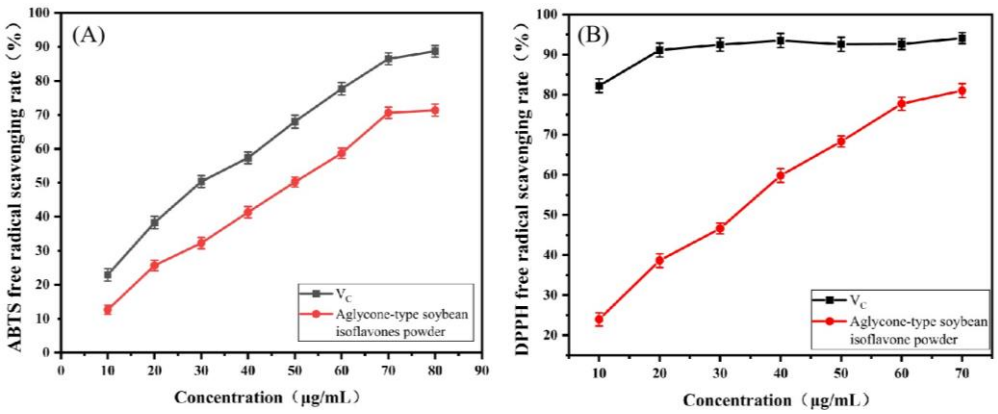

Figure 6. In vitro antioxidant activity. (**A**) ABTS, (**B**) DPPH.

3.4.2. CNS Protection in Zebrafish

The MTC of the aglycone-type soy isoflavone sample was 500 μg/mL. At 1000 μg/mL and 2000 μg/mL, zebrafish mortality increased to 20% and 100%, respectively, demonstrating significant toxicity. Based on safety considerations, subsequent experiments utilized test concentrations of 125, 250, and 500 μg/mL to investigate neuroprotective effects (Table 4).

To investigate the protective effects of various concentrations of aglycone soy isoflavones on the CNS of zebrafish damaged by MMF, AO fluorescence was utilized to label apoptotic cells within the neural axis. By selectively staining the condensed chromatin of the apoptotic cells with bright green fluorescence, the apoptotic cells were distinguished from living cells. Compared with those in the control group, significantly fewer apoptotic cells were observed in the aglycone soy isoflavone treatment group (Figure 7). This suggests that aglycone soy isoflavones may exert neuroprotective effects by inhibiting apoptosis.

Table 4. Central nervous system-protective effect concentration exploration (n = 30).

Constituencies	Concentration (μg/mL)	Deaths (tail)	Mortality (%)	Phenotype
Normal control group	-	0	0	No significant abnormalities were observed
Model control group	-	0	0	No significant abnormalities were observed
Aglycone soy isoflavone samples	125	0	0	The status was similar to that of the model control group
	250	0	0	The status was similar to that of the model control group
	500	0	0	The status was similar to that of the model control group
	1000	6	20	-
	2000	30	100	-

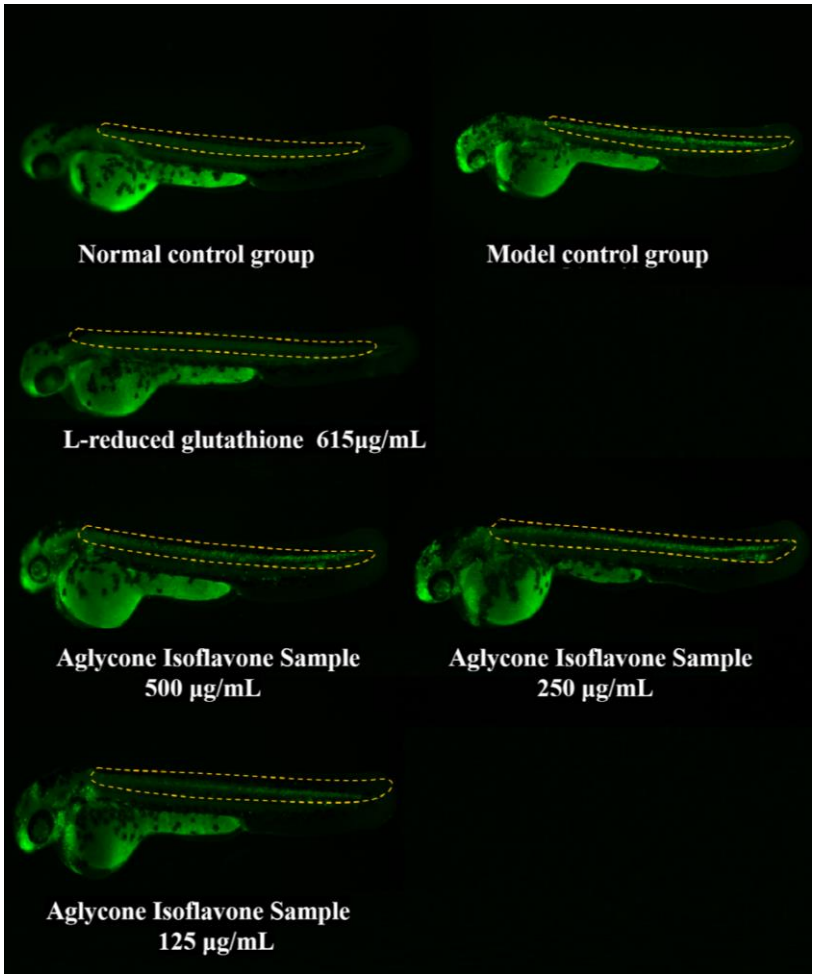

Figure 7. Fluorescence intensity of zebrafish neural axis cell apoptosis after sample treatment (Magnification 30 times). Note: The yellow dashed box indicates the analyzed portion of the neural axis (the green particles represent apoptotic cells).

The protective rates of 125, 250, and 500 μg/mL aglycone soy isoflavones on the zebrafish CNS were 27.20 ± 0.09%, 33.94 ± 0.08%, and 76.58 ± 1.07%, respectively (Table 5). Hence, the protective effect of aglycone soy isoflavones on the zebrafish CNS significantly increased with concentration, particularly at 500 μg/mL, where the protection was most pronounced compared with that of the model control group ($p < 0.001$). At 500 μg/mL, the

aglycone soy isoflavones notably mitigated the CNS damage elicited by MMF, showcasing a protective efficacy akin to that observed in the positive control group treated with glutathione, with no statistical difference. This suggests that aglycone soy isoflavones may offer protective effects from CNS damage in zebrafish comparable to glutathione. This mechanism of action may involve the capacity of aglycone soy isoflavones to effectively reduce apoptosis in neural axis cells, providing substantial protection for the CNS.

Table 5. Central nervous protection of samples (n = 30).

Constituencies	Concentration (μg/mL)	Neuraxial Apoptosis Fluorescence Intensity (Pixel, Mean ± SE)	CNS Protection Rate (%)
Normal control group	-	81,656 ± 2131 ***	
Model control group	-	162,661 ± 6501	
Glutathione	615	107,491 ± 5303 ***	68.11 ± 0.27
Aglycone-type soybean isoflavone sample	125	140,627 ± 6099	27.20 ± 0.09
	250	135,166 ± 6174	33.94 ± 0.08
	500	100,628 ± 1809 ***	76.58 ± 1.07

Note: ***: $p < 0.001$ compared with the model control group.

The core CNS protection mechanisms elicited by aglycone soy isoflavones are hypothesized to involve anti-apoptotic and antioxidant effects [36]. These compounds may inhibit the apoptosis of neural axis cells by regulating apoptosis-related proteins such as Bax/Bcl-2 [37], which will be a key focus of our subsequent experiments. Additionally, the phenolic hydroxyl groups in these compounds may enhance their free radical scavenging capacity. The variations in the effects of aglycone soy isoflavone standards and pure products may result from differences in purity or isomer composition. Clarifying the contributions of active components through compositional analysis will also be part of our future work. Our findings are consistent with the existing literature on the CNS-protective effects of soy isoflavone compounds [38]. However, given the limitations of the zebrafish model, our next research focus will be the use of rodents (such as Kunming mice and Sprague Dawley mice) as mammalian models to further verify the ability of aglycone soy isoflavones products to penetrate the blood–brain barrier.

4. Conclusions

Under optimal conditions, using soybean sprout powder as the raw material and employing a combination of hydrolytic enzymes with varying specificities and mechanisms of action (β-glucosidase, cellulase, hemicellulase, and β-galactosidase) facilitates the conversion of up to 97% of the glycoside soy isoflavones in the raw material into more bioactive aglycone soy isoflavones. Furthermore, under optimal purification conditions, a soy isoflavone product with a high aglycone content and relatively high purity can be prepared. Aglycone soy isoflavones also exhibit high capacities for scavenging DPPH and ABTS radicals in vitro, demonstrating antioxidant activity comparable to synthetic antioxidants. Importantly, aglycone soy isoflavone samples exhibit CNS-protective effects in zebrafish. Consequently, high-purity aglycone soy isoflavones, obtained through bioenzymatic treatments, can serve as greener and healthier additives in food, health products, and cosmetics.

Future research should focus on investigating the synergistic mechanisms of the enzyme complex, developing more efficient and cost-effective enzyme formulations, and implementing methods to improve the stability and bioavailability of aglycone soy isoflavones to enhance their widespread application.

Supplementary Materials: The following supporting information can be downloaded at https://www.mdpi.com/article/10.3390/pr13061831/s1, Table S1: Elution program of mobile phase; Table S2: Linear regression equation of soybean isoflavone; Table S3: Analysis of variance (ANOVA) for regression model.

Author Contributions: Conceptualization, Y.Z. and J.X.; methodology, Y.Z.; software, Y.Z., Y.F., and P.D.; validation, Y.Z., Y.F., L.H., and Y.L.; formal analysis, P.D. and N.L.; investigation, L.H., W.L., and N.L.; resources, J.X.; data curation, Y.Z. and Y.F.; writing—original draft preparation, Y.Z.; writing—review and editing, P.D. and N.L.; visualization, Y.F., L.H., and W.L.; supervision, P.D.; project administration, J.X.; funding acquisition, J.X. All authors have read and agreed to the published version of the manuscript.

Funding: This research was funded by the Key Research and Development Program of Shandong Province (2022CXGC020801).

Institutional Review Board Statement: The animal study protocol was approved by the by the Animal Ethics Committee of the Qilu University of Technology (Approval No. 2024-003, 10 September 2024).

Informed Consent Statement: Not applicable.

Data Availability Statement: The data are contained within the article and Supplementary Materials.

Acknowledgments: This work was supported by the State Key Laboratory of Green Papermaking and Resource Recycling at the Qilu University of Technology. We thank them for their help and support, as well as the funding received from the Key R&D Program of Shandong Province.

Conflicts of Interest: Authors Yanhong Fu, Lizhen Hao, and Wenlong Liu are employed by Shandong Loncote Enzymes Co., Ltd. The remaining authors declare that the research was conducted in the absence of any commercial or financial relationships that could be construed as a potential conflict of interest.

Abbreviations

The following abbreviations are used in this manuscript:

ABTS	2,2′-Azinobis
AO	Acridine orange
CNS	Central nervous system
D	Daidzin
DE	Daidzein
DPPH	1,1-Diphenyl-2-picrylhydrazyl
G	Glycitin
GE	Glycitein
GL	Genistin
GLE	Genistein
IMPDH	Inosine monophosphate dehydrogenase
MMF	Mycophenolate mofetil
MTC	Maximum test concentration
V_C	Vitamin C

References

1. Leuner, O.; Havlik, J.; Hummelova, J.; Prokudina, E.; Novy, P.; Kokoska, L. Distribution of isoflavones and coumestrol in neglected tropical and subtropical legumes. *J. Sci. Food Agric.* **2013**, *93*, 575–579. [CrossRef] [PubMed]
2. Chen, L.R.; Chen, K.H. Utilization of isoflavones in soybeans for women with menopausal syndrome: An overview. *Int. J. Mol. Sci.* **2021**, *22*, 3212. [CrossRef] [PubMed]
3. Wang, S.Y.; Zhang, Y.J.; Zhu, G.Y.; Shi, X.C.; Chen, X.; Herrera-Balandrano, D.D.; Liu, F.Q.; Laborda, P. Occurrence of isoflavones in soybean sprouts and strategies to enhance their content: A review. *J. Food Sci.* **2022**, *87*, 1961–1982. [CrossRef]

4. Uddin, M.S.; Kabir, M.T. Emerging signal regulating potential of genistein against Alzheimer's disease: A promising molecule of interest. *Front. Cell Dev. Biol.* **2019**, *7*, 197. [CrossRef]
5. Hu, C.; Wong, W.T.; Wu, R.; Lai, W.F. Biochemistry and use of soybean isoflavones in functional food development. *Crit. Rev. Food Sci. Nutr.* **2020**, *60*, 2098–2112. [CrossRef]
6. Pei, R.; Zhang, J.; Tian, L.; Zhang, S.; Han, F.; Yan, S.; Wang, L.; Li, B.; Sun, J. Identification of novel QTL associated with soybean isoflavone content. *Crop J.* **2018**, *6*, 244–252. [CrossRef]
7. Wang, Q.; Ge, X.; Tian, X.; Zhang, Y.; Zhang, J.; Zhang, P. Soy isoflavone: The multipurpose phytochemical (Review). *Biomed. Rep.* **2013**, *1*, 697–701. [CrossRef] [PubMed]
8. Lee, C.H.; Yang, L.; Xu, J.Z. Relative antioxidant activity of soybean isoflavones and their glycosides. *Food Chem.* **2005**, *90*, 735–741. [CrossRef]
9. Chen, P.; Sun, J.W.; Liang, Z.Q.; Xu, H.; Du, P.; Li, A.; Meng, Y.; Reshetnik, E.I.; Liu, L.; Li, C. The bioavailability of soy isoflavones in vitro and their effects on gut microbiota in the simulator of the human intestinal microbial ecosystem. *Food Res. Int.* **2022**, *152*, 110868. [CrossRef]
10. Wójciak, M.; Drozdowski, P.; Skalska-Kamińska, A.; Zagórska-Dziok, M.; Ziemlewska, A.; Nizioł-Łukaszewska, Z.; Latalska, M. Protective, anti-inflammatory, and anti-aging effects of soy isoflavones on skin cells: An overview of in vitro and in vivo studies. *Molecules* **2024**, *29*, 5790. [CrossRef]
11. Lee, J.H.; Choung, M.G. Determination of optimal acid hydrolysis time of soybean isoflavones using drying oven and microwave assisted methods. *Food Chem.* **2011**, *129*, 577–582. [CrossRef]
12. Sun, X.D. Enzymatic hydrolysis of soy proteins and the hydrolysates utilisation. *Int. J. Food Sci. Technol.* **2011**, *46*, 2447–2459. [CrossRef]
13. Chien, H.J.; Wang, C.S.; Chen, Y.H.; Toh, J.T.; Zheng, Y.F.; Hong, X.G.; Lin, H.Y.; Lai, C.C. Rapid determination of isoflavones and other bioactive compounds in soybean using SWATH-MS. *Anal. Chim. Acta* **2020**, *1103*, 122–133. [CrossRef]
14. Silva, M.B.R.; Falcão, H.G.; Kurozawa, L.E.; Prudencio, S.H.; de Camargo, A.C.; Shahidi, F.; Ida, E.I. Ultrasound and hemicellulase-assisted extraction increase β-glucosidase activity, the content of isoflavone aglycones and antioxidant potential of soymilk. *J. Food Bioact.* **2019**, *6*, 140–147. [CrossRef]
15. Otieno, D.O.; Ashton, J.F.; Shah, N.P. Isoflavone phytoestrogen degradation in fermented soymilk with selected β-glucosidase producing L. acidophilus strains during storage at different temperatures. *Int. J. Food Microbiol.* **2007**, *115*, 79–88. [CrossRef] [PubMed]
16. Zhang, E.J.; Ng, K.M.; Luo, K.Q. Extraction and purification of isoflavones from soybeans and characterization of their estrogenic activities. *J. Agric. Food Chem.* **2007**, *55*, 6940–6950. [CrossRef]
17. Nemitz, M.C.; Moraes, R.C.; Koester, L.S.; Bassani, V.L.; von Poser, G.L.; Teixeira, H.F. Bioactive soy isoflavones: Extraction and purification procedures, potential dermal use and nanotechnology-based delivery systems. *Phytochem. Rev.* **2015**, *14*, 849–869. [CrossRef]
18. Chea, J.D.; Lehr, A.L.; Stanzione, J.F., III; Yenkie, K.M. Evaluation of isoflavone extraction options at commercial scale. *Biofuel Bioprod. Biorefin.* **2022**, *16*, 1708–1725. [CrossRef]
19. Xi, L.; Mu, T.; Sun, H. Preparative purification of polyphenols from sweet potato (*Ipomoea batatas* L.) leaves by AB-8 macroporous resins. *Food Chem.* **2015**, *172*, 166–174. [CrossRef]
20. Yang, Q.; Zhao, M.; Lin, L. Adsorption and desorption characteristics of adlay bran free phenolics on macroporous resins. *Food Chem.* **2016**, *194*, 900–907. [CrossRef]
21. Dong, Y.; Zhao, M.; Sun-Waterhouse, D.; Zhuang, M.; Chen, H.; Feng, M.; Lin, L. Absorption and desorption behaviour of the flavonoids from *Glycyrrhiza glabra* L. leaf on macroporous adsorption resins. *Food Chem.* **2015**, *168*, 538–545. [CrossRef]
22. Chang, X.L.; Wang, D.; Chen, B.Y.; Feng, Y.M.; Wen, S.H.; Zhan, P.Y. Adsorption and desorption properties of macroporous resins for anthocyanins from the calyx extract of roselle (*Hibiscus sabdariffa* L.). *J. Agric. Food Chem.* **2012**, *60*, 2368–2376. [CrossRef] [PubMed]
23. Yu, X.; Meenu, M.; Xu, B.; Yu, H. Impact of processing technologies on isoflavones, phenolic acids, and antioxidant capacities of soymilk prepared from 15 soybean varieties. *Food Chem.* **2021**, *345*, 128612. [CrossRef] [PubMed]
24. Szeja, W.; Grynkiewicz, G.; Rusin, A. Isoflavones, their glycosides and glycoconjugates. Synthesis and biological activity. *Curr. Org. Chem.* **2017**, *21*, 218–235. [CrossRef] [PubMed]
25. Vitale, D.C.; Piazza, C.; Melilli, B.; Drago, F.; Salomone, S. Isoflavones: Estrogenic activity, biological effect and bioavailability. *Eur. J. Drug Metab. Pharmacokinet.* **2013**, *38*, 15–25. [CrossRef]
26. Zhang, X.; Veliky, C.V.; Birru, R.L.; Barinas-Mitchell, E.; Magnani, J.W.; Sekikawa, A. Potential protective effects of equol (soy isoflavone metabolite) on coronary heart diseases—From molecular mechanisms to studies in humans. *Nutrients* **2021**, *13*, 3739. [CrossRef]

27. De Camargo, A.C.; Favero, B.T.; Morzelle, M.C.; Franchin, M.; Alvarez-Parrilla, E.; de la Rosa, L.A.; Geraldi, M.V.; Maróstica Júnior, M.R.; Shahidi, F.; Schwember, A.R. Is chickpea a potential substitute for soybean? Phenolic bioactives and potential health benefits. *Int. J. Mol. Sci.* **2019**, *20*, 2644. [CrossRef]
28. Wang, W.-L.; Chen, S.-M.; Lee, Y.-C.; Chang, W.-W. Stigmasterol inhibits cancer stem cell activity in endometrial cancer by repressing IGF1R/mTOR/AKT pathway. *J. Funct. Foods.* **2022**, *99*, 105338. [CrossRef]
29. Popović, D.B.; Sinkjær, T. Central nervous system lesions leading to disability. *J. Autom. Control* **2008**, *18*, 11–23. [CrossRef]
30. Jurisch-Yaksi, N.; Yaksi, E.; Kizil, C. Radial glia in the zebrafish brain: Functional, structural, and physiological comparison with the mammalian glia. *Glia* **2020**, *68*, 2451–2470. [CrossRef]
31. Jiang, L.-L.; Liu, M.-H.; Li, J.-Y.; He, Z.-H.; Li, H.; Shen, N.; Wei, P.; He, M.-F. Mycophenolic acid-induced developmental defects in zebrafish embryos. *Int. J. Toxicol.* **2016**, *35*, 712–718. [CrossRef]
32. Magiera, S.; Sobik, A. Ionic liquid-based ultrasound-assisted extraction coupled with liquid chromatography to determine isoflavones in soy foods. *J. Food Compos. Anal.* **2017**, *57*, 94–101. [CrossRef]
33. Macedo, G.A.; Caria, C.R.E.P.; Barbosa, P.P.M.; Mazine, M.R.; Gambero, A. Bioaccessibility evaluation of soymilk isoflavones with biotransformation processing. *Foods* **2023**, *12*, 3401. [CrossRef] [PubMed]
34. Kim, M.S.; Jung, Y.S.; Jang, D.; Cho, C.H.; Lee, S.H.; Han, N.S.; Kim, D.O. Antioxidant capacity of 12 major soybean isoflavones and their bioavailability under simulated digestion and in human intestinal Caco-2 cells. *Food Chem.* **2022**, *374*, 131493. [CrossRef]
35. Lee, D.P.S.; Gan, A.X.; Kim, J.E. Incorporation of biovalorised okara in biscuits: Improvements of nutritional, antioxidant, physical, and sensory properties. *LWT* **2020**, *134*, 109902. [CrossRef]
36. Ma, W.; Ding, B.; Yu, H.; Yuan, L.; Xi, Y.; Xiao, R. Genistein alleviates β-amyloid-induced inflammatory damage through regulating toll-like receptor 4/nuclear factor κ B. *J. Med. Food* **2015**, *18*, 273–279. [CrossRef]
37. Zhang, Y.; Yin, L.; Dong, J.; Xia, X. Soy isoflavones protect neuronal PC12 cells against hypoxic damage through Nrf2 activation and suppression of p38 MAPK and AKT–mTOR pathways. *Antioxidants* **2022**, *11*, 2037. [CrossRef] [PubMed]
38. Kim, I.S. Current perspectives on the beneficial effects of soybean isoflavones and their metabolites for humans. *Antioxidants* **2021**, *10*, 1064. [CrossRef]

Disclaimer/Publisher's Note: The statements, opinions and data contained in all publications are solely those of the individual author(s) and contributor(s) and not of MDPI and/or the editor(s). MDPI and/or the editor(s) disclaim responsibility for any injury to people or property resulting from any ideas, methods, instructions or products referred to in the content.